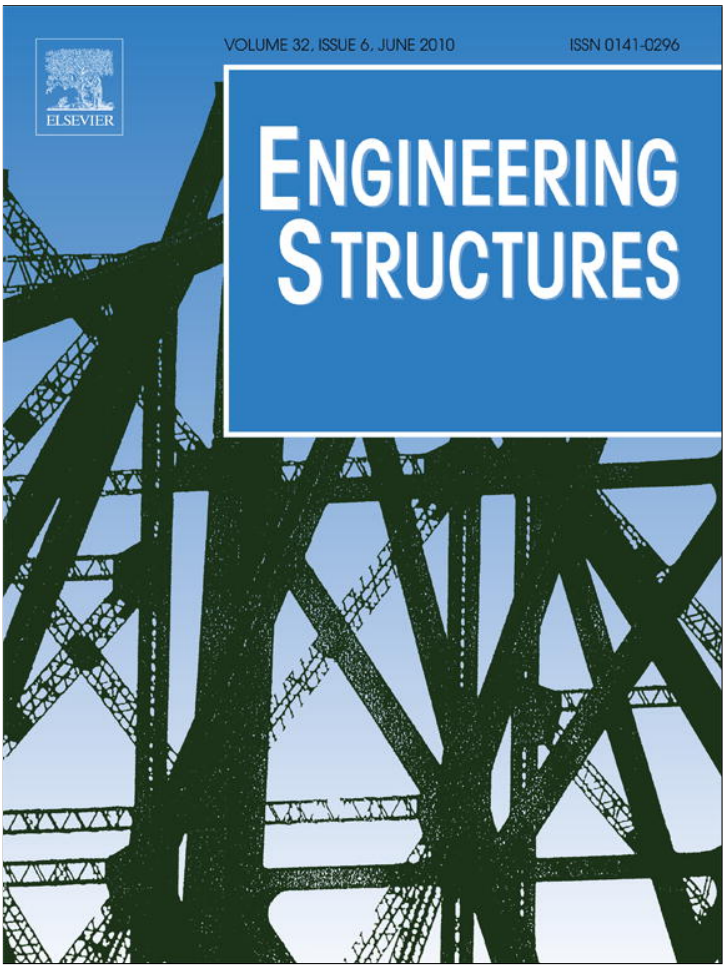

Engineering Structures 32 (2010) 1547–1555

Contents lists available at ScienceDirect

Engineering Structures

journal homepage: www.elsevier.com/locate/engstruct

Fragility analysis of steel moment frames with various seismic connections subjected to sudden loss of a column

Junhee Park [a], Jinkoo Kim [b,*]

[a] Korea Atomic Energy Research Institute, Daejeon, Republic of Korea

[b] Department of Architectural Engineering, Sungkyunkwan University, Suwon, Republic of Korea

ARTICLE INFO

Article history:
Received 29 June 2009
Received in revised form
25 January 2010
Accepted 1 February 2010
Available online 7 March 2010

Keywords:
Seismic connections
Progressive collapse
Pushdown analysis
Fragility curve

ABSTRACT

In this study the progressive collapse potential of steel structures having WUFB, RBS, and WCPF connections was investigated considering the uncertainty in material properties such as yield strength, live load, and elastic modulus. The beam-end rotation was used as a member-level limit state for progressive collapse. Pushdown analyses of the model structure with three different connection types were carried out after removing one of the first-story columns. Fragility curves were obtained based on the probability of exceeding a given limit state for vertical displacement using the First-Order Second Moment (FOSM) method. The analysis results showed that the RBS connections showed the highest load resisting capacity against collapse due to their highly ductile behavior and that the loss of an exterior column turned out to be more vulnerable for progressive collapse than the loss of an interior column.

1. Introduction

Progressive collapse refers to the phenomenon whereby local damage of structural elements caused by abnormal loads results in global collapse of the structure. An abnormal load includes any loading condition that is not considered in normal design process but may cause significant damage to structures. The potential abnormal loads that can trigger progressive collapse are categorized as: aircraft impact, design/construction error, fire, gas explosions, accidental overload, hazardous materials, vehicular collision, bomb explosions, etc. [1]. For a realistic simulation of progressive collapse, the analysis process needs to include uncertain characteristics of material properties. Nevertheless, most recent studies on progressive collapse of building structures have been conducted based on deterministic approaches where the nominal or average values of the design parameters were used [2–7]. However, the progressive collapse mechanism and the capacity of structures can be affected by probabilistic properties of the design parameters and load combinations. An application of the theory of probability to the structural analysis is one of the ways to deal with uncertain material properties which are considered as random variables.

In structural engineering field a conditional probability of exceeding a limit state is generally expressed by fragility curves. Fragility analyses have been successfully carried out to investigate seismic vulnerability of various structures [8–12]. In this study fragility analyses were carried out to investigate the progressive collapse potential of steel structures with 'welded unreinforced flange-bolted web' (WUF-B), 'reduced beam section' (RBS), and 'welded cover-plated flange' (WCPF) connections considering the uncertainty of design variables such as yield strength, live load, and elastic modulus. The beam-end rotation was used as a criterion for initiation of progressive collapse. Pushdown analyses of the model structure were carried out after removing one of the first-story columns. Fragility curves were obtained based on the probability of exceeding a given limit state for vertical displacement using the First-Order Second Moment (FOSM) method.

2. Procedure for drawing fragility curves

2.1. Limit states for progressive collapse

The GSA guidelines for progressive collapse [13] regulate that the maximum allowable extents of collapse resulting from the instantaneous removal of a column shall be confined to the structural bays directly above the instantaneously removed column as shown in Fig. 1. Any structural failure outside of the allowable extents is defined as the occurrence of progressive collapse. Table 1 shows the limit states specified in the FEMA-356 [14] for various seismic connections.

2.2. Probability of collapse

Building failures can result from a multiplicity of hazards, such as occupancy loads and other demands, misuse, extreme

* Corresponding author. Tel.: +82 31 290 7560; fax: +82 31 290 7570.
E-mail address: jkim12@skku.edu (J. Kim).

0141-0296/$ – see front matter © 2010 Elsevier Ltd. All rights reserved.
doi:10.1016/j.engstruct.2010.02.003

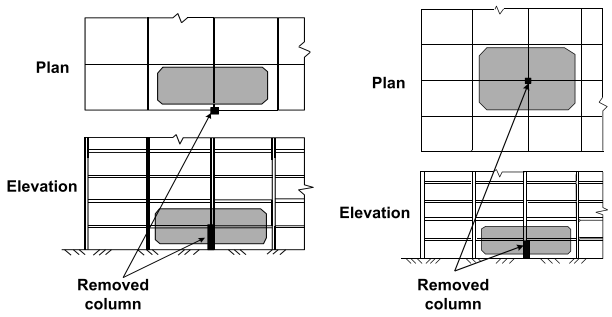

(a) Exterior consideration. (b) Interior consideration.

Fig. 1. Maximum allowable collapse areas (GSA 2003).

Table 1
Limit states for seismic connections specified in FEMA-356 (d: beam depth; IO: Immediate occupancy; LS: Life safety; and CP: Collapse prevention).

Connection type	Limit states		
	IO	LS	CP
WUF	0.0128–0.0003d	0.0337–0.0009d	0.0284–0.0004d
RBS	0.0125–0.0001d	0.0380–0.0002d	0.0500–0.0003d
WCPF	0.0078	0.0177	0.0236

environmental effects, fires, and other abnormal loads. If each of these distinct hazards is represented by an event, H, and if simply local damage rather than a damage state is specified, then the total probability of structural collapse $P(C)$ due to the event H can be represented as:

$$P(C) = P(C|LD)P(LD|H)P(H) \tag{1}$$

in which $P(H)$ = probability of hazard H, $P(LD|H)$ = probability of local damage given that H occurs, and $P(C|LD)$ = probability of collapse given that hazard and local damage both occur. In this study the probability of hazard and the probability of local damage caused by the hazard were assumed to be 1.0, and only the probability of collapse given the occurrence of the hazard and the local damage was considered for simplicity.

2.3. Damage index

To express a damage state of a structural element, Powell and Allahabadi [7] proposed the following damage model:

$$D = \frac{u_{\max} - u_y}{u_{\min} - u_y} \tag{2}$$

where $u_{\max}$ is the maximum displacement, $u_{\min}$ is the maximum displacement under monotonic load, and u_y is the yield displacement. In this study the above damage index was modified as follows to express damage state under progressive collapse:

$$D = \frac{u_{\max}}{u_{\min}} \tag{3}$$

where $u_{\lim}$ and $u_{\max}$ represent the displacement at limit state and the maximum displacement response, respectively.

2.4. Fragility curves

The fragility curve for seismic load is generally drawn based on a system-level limit state such as inter-story drift. In this study the vertical deflection at the maximum beam rotation caused by the sudden removal of a column was defined as the limit state for system-level collapse to obtain fragility curve. The mean and standard deviation of vertical deflection were obtained based on the probability distribution of design variables using the First-Order Second Moment (FOSM). The fragility curve was drawn using the probability of collapse obtained from the probability of the maximum deflection exceeding the limit state. Fig. 2 depicts the procedure for drawing the fragility curve of a structure with a column suddenly removed.

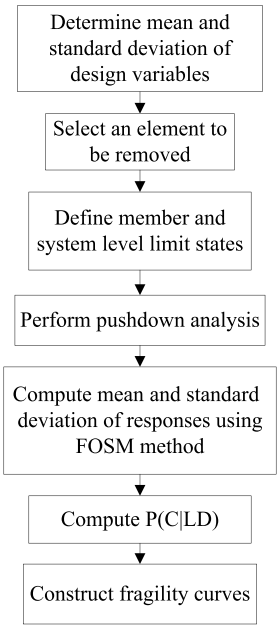

Fig. 2. Procedure for deriving fragility curves.

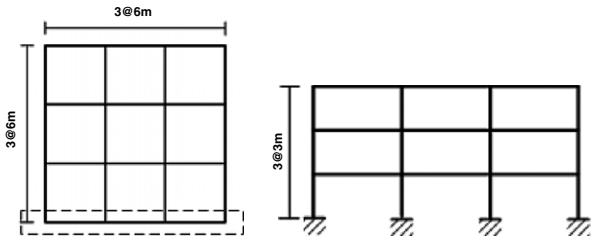

(a) Plan. (b) Elevation.

Fig. 3. Analysis model structure.

3. Analysis model structures

3.1. Design of analysis models

The prototype structure for an analysis model is a three-bay, three-story steel moment resisting frame as shown in Fig. 3. The structure was designed with dead and live loads of 5 kN/m^2 and 2.5 kN/m^2, respectively, and seismic load with S_{Ds} and S_{D1} equal to 0.36 g and 0.15 g, respectively, with the response modification factor of 6.0. The interior and exterior columns were designed with H300 × 300 × 10 × 16 and H250 × 250 × 14 × 14, respectively, and beams were designed with H300 × 120 × 8 × 13. The beams and columns were made of SS400 and SM490 steel, respectively. The panel zone flexibility was considered in the analysis model of beam–column joints based on the work of Krawinkler et al. [15]. As an analysis model the exterior frame enclosed in the dotted rectangle in Fig. 1 was analyzed using the nonlinear analysis program code OpenSees [16]. The beams and columns were modeled using the nonlinear beam–column elements with five integration points and 2% of post-yield stiffness. The catenary action of a beam caused by large deflection was considered using the 'Corotational' option in the OpenSees. For initiation of progressive collapse, one of the corner columns or interior columns was suddenly removed one at a time as shown in Fig. 4.

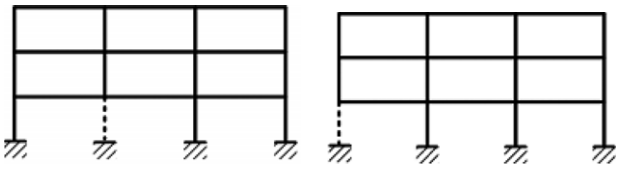

(a) Removal of an interior column. (b) Removal of an exterior column.

Fig. 4. Location of a removed column.

3.2. Modeling of connections and definition of limit states

In the model structure three types of seismic connections were applied: WUFB (welded unreinforced flange-bolted web connections), WCPF (welded cover-plated flanges), and RBS (reduced beam section). Fig. 5 shows the analysis modeling of each connection type. For modeling of the WUFB connections, a uniform beam cross-sectional dimension was used, whereas in RBS connections, which were developed after the Northridge Earthquake, the equivalent cross-sectional dimension proposed by Lee [17] was used to accommodate the effect of the reduced cross-sectional area at beam ends. The cross-sectional areas at beam ends were increased in order to model the WCPF connections as shown in Fig. 5(c).

The limit states for beam-end rotation under monotonic loading are expected to be larger than those under cyclic earthquake loads. Therefore it seems to be reasonable that the limit states for WUFB and WCPF connections specified in the GSA guidelines for progressive collapse are slightly larger than those specified in the FEMA-356 [8] for collapse prevention limit state. However the DoD limit state for the RBS connection is 33% less than that of the FEMA-356 value. Kim et al. [18] showed that the maximum rotation angle of a beam–column subassemblage with RBS connection subjected to a monotonically increasing load was twice and three times as large as those specified in the FEMA-356 and DoD guidelines, respectively. In this paper the limit states of seismic connections given in the FEMA-356 were mainly used to define failure of connections because it provides more detailed limit states for steel beam sections considering variation of beam depth. Table 1 shows the limit states for seismic connections specified in FEMA-356.

4. Nonlinear static analysis results

Fig. 6 shows the nonlinear static pushdown analysis results of the model structure with various connection types. Mean values of design variables were used to model the structure. Displacement-controlled pushdown analysis was carried out with a first-story column removed. The horizontal and the vertical axes represent the vertical displacement and the load factor, respectively. The load factor of 2.0 corresponds to the state in which the applied vertical load reached the load specified in the GSA guideline, 2(deadload + 0.25 × liveload). The maximum load factor of less than 2.0 implies that the structure may collapse as a result of removing one of the columns. The filled circles, triangles, and squares marked on the pushdown curves represent the vertical displacements corresponding to the IO (Immediate Occupancy), LS (Life Safety), and CP (Collapse Prevention) limit states, respectively. The shown limit states are not the element-level limit states, but are the system-level limit states defined in the GSA guideline at which the maximum rotation of an element located outside of the allowable collapse area, as described in Fig. 1, exceeds the limit state shown in Table 1. Table 2 presents the maximum vertical displacement, plastic hinge rotation, and load factors at each limit state of the model structure with different connection types when an interior column was removed. It can be seen in Fig. 6 that the model structure with WCPF connections showed the highest strength, whereas the structure with RBS connections showed the lowest strength when a first-story column was removed. However, the structure with RBS connections actually had the largest ductility before failure. This resulted in the highest load factor of the structure with RBS connections at CP limit state as shown in Table 2. It also can be observed that the maximum strengths increased further when an internal column was removed than when an external column was removed. This implies that the progressive collapse potential of the structure with a missing exterior column is higher than that of the structure with a missing interior column.

Figs. 7–9 plot the plastic hinge formation of the model structure with different connection types at each limit state when an interior column is removed. It can be observed that plastic hinges formed first at the second-story beam of the interior span and propagated to the beams in the roof and in the exterior span. No plastic hinge was observed in the columns. The largest number of plastic hinges occurred in the structure with RBS connections.

5. Fragility analysis

5.1. Variation of design variables

It was observed that the progressive collapse resisting capacity of building structures was sensitive to the variation of design variables [19]. Table 3 shows the statistical data for some selected design variables, such as yield strengths of beams and columns, live load, and elastic modulus [20–22]. The correlation coefficients between the design variables to be used to compute the covariance are shown in Table 4.

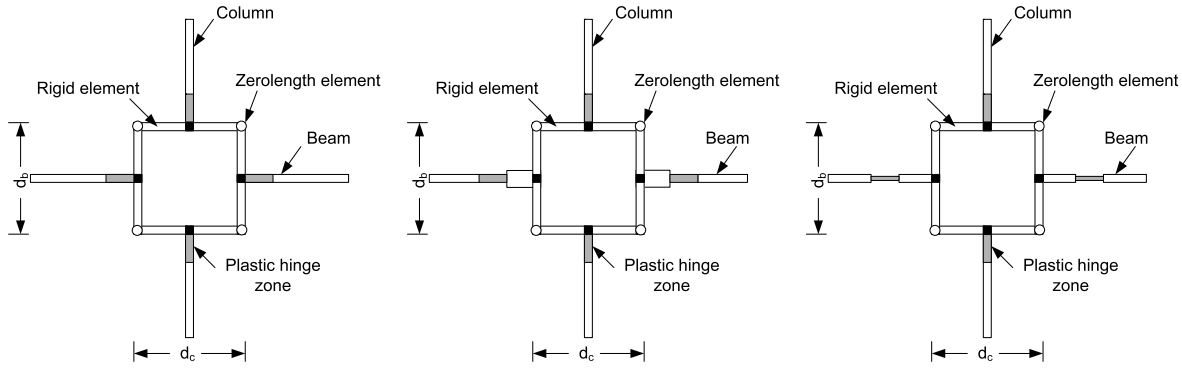

(a) WUFB. (b) WCPF. (c) RBS.

Fig. 5. Modeling of beam–column joints.

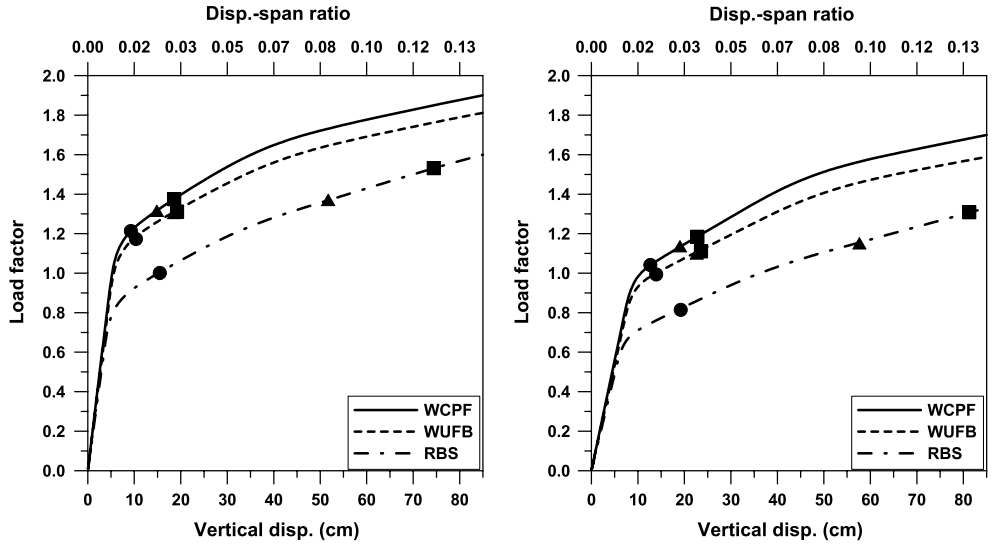

(a) Removal of an interior column. (b) Removal of an exterior column.

Fig. 6. Pushdown curves of the model structure with various connection types.

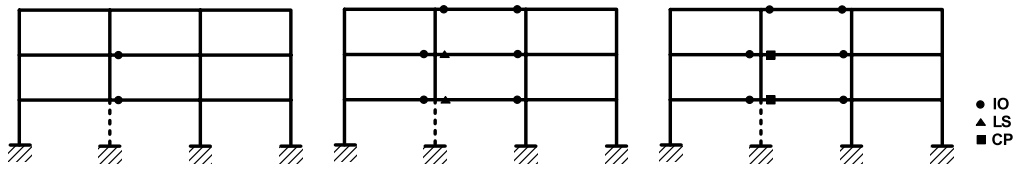

(a) IO stage. (b) LS stage. (c) CP stage.

Fig. 7. Plastic hinge formation at each limit state (WUFB connections).

Table 2
Maximum responses and load factors at each limit state of model structure with different connection types when an interior column was removed.

Connection type	Plastic hinge rotation (rad)	Load factor	Max. displacement (cm)	Limit states
WUFB	0.0093	1.1844	10.30	IO
	0.0231	1.3128	18.75	LS
	0.0237	1.3174	19.10	CP
WCPF	0.0078	1.2158	9.35	IO
	0.0177	1.3201	15.05	LS
	0.0236	1.3752	18.55	CP
RBS	0.0113	1.0037	15.40	IO
	0.0357	1.3711	51.95	LS
	0.0465	1.5311	74.45	CP

Table 3
Statistical data for design variables (Unit: kN, cm).

Variables	Mean	Standard deviation	Coefficient of variation (%)	Probability distribution
Beam yield strength	23.5	1.24	5.28	Lognormal
Column yield strength	32.5	3.28	10.10	Lognormal
Live load	0.000274	0.0000488	17.83	Lognormal
Elastic modulus	20594.0	679.602	3.30	Normal

Table 4
Correlation coefficients for design variables.

Variables	Beam yield strength	Column yield strength	Live load	Elastic modulus
Beam yield strength	1.0	0.8	0.0	0.2
Column yield strength	0.8	1.0	0.0	0.2
Live load	0.0	0.0	1.0	0.0
Elastic modulus	0.2	0.2	0.0	1.0

5.2. Variation of vertical displacement

In this study the First-Order Second Moment (FOSM) method was applied to obtain the probabilistic distribution of design variables. In the FOSM method, means and standard deviations of random variables are assumed and the mean and standard deviations of structural responses are obtained. The advantage of the FOSM method is that the analysis procedure is simpler than

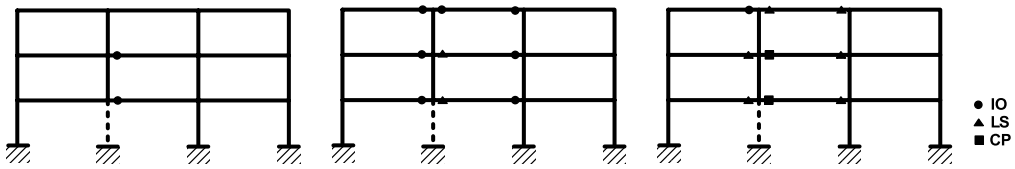

(a) IO stage. (b) LS stage. (c) CP stage.

Fig. 8. Plastic hinge formation at each limit state (WCPF connections).

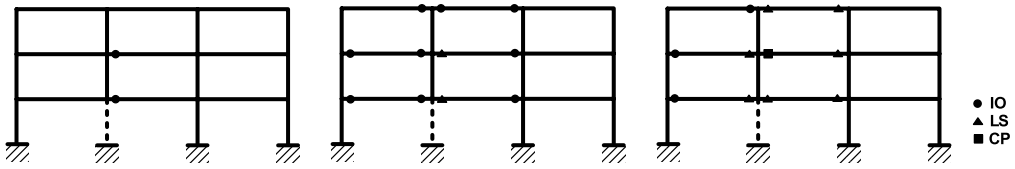

(a) IO stage. (b) LS stage. (c) CP stage.

Fig. 9. Plastic hinge formation at each limit state (RBS connections).

rigorous probabilistic methods such as the first-order reliability method, stochastic finite element method, and the Monte Carlo simulation method, while major probabilistic properties of the structural responses can be obtained accurately enough. Let us assume that a random variable $X = (x_1, x_2, \ldots, x_n)^T$ has mean and co-variance vectors $\mu_X = (\mu_1, \mu_2, \ldots, \mu_n)^T$ and $VC[X]$, respectively. The first-order approximation of a function $Y = g(X)$ using Taylor series expansion evaluated at x_0 can be given as

$$Y \approx g_0 + \left(\frac{dg}{dx}\right)_0 (X - x_0) \tag{4}$$

where $()_0$ denotes a function evaluated at x_0. In the formulation the random variable X can be considered as the structural design parameters and the function $Y = g(X)$ represents the structural analysis and the corresponding responses. The mean μ_Y and the standard deviation σ_Y of $Y = g(X)$ can be approximated using Eq. (4) as

$$\mu_Y = E[g(X)] \approx g_0 + \left(\frac{dg}{dx}\right)_0 (\mu_X - x_0) \tag{5}$$

$$\sigma_Y^2 = E\left[g^2(X)\right] - \mu_Y^2 \approx g_0^2 + \left(\frac{dg}{dx}\right)_0^2 \sigma_X^2 + 2g_0\left(\frac{dg}{dx}\right)_0 (\mu_X - x_0) - \mu_Y^2. \tag{6}$$

For $x_0 = \mu_X$ Eqs. (5) and (6) can be approximated using the FOSM method as follows [15]:

$$\mu_Y \approx g(\mu_X) \tag{7}$$

$$\sigma_Y^2 \approx \left(\frac{dg}{dx}\right)_0^2 \sigma_X^2. \tag{8}$$

Let us consider the functions $Y = g(X)$, $Y_1 = g(X_1, \mu_2, \mu_3, \ldots, \mu_n)$, $Y_2 = g(\mu_1, X_2, \mu_3, \ldots, \mu_n)$, and $Y_n = g(\mu_1, \mu_2, \ldots, \mu_{n-1}, X_n)$. The mean and standard deviation approximated by the FOSM method are

$$\mu_Y = \mu_{Yi} \approx g(\mu_1, \mu_2, \ldots, \mu_n) = g(\mu_X) \quad i = 1, 2, \ldots, n \tag{9}$$

$$\sigma_Y^2 \approx \nabla^T g(X) VC(X) \nabla g(X) \tag{10}$$

$$\sigma_{Yi}^2 \approx \left(\frac{\partial g}{\partial xi}\right)_0^2 \sigma_i^2 \quad i = 1, 2, \ldots, n \tag{11}$$

where $\nabla g(X) = [\partial g/\partial x_1, \partial g/\partial x_2, \ldots, \partial g/\partial x_n]^T$ is the partial differential of $g(X)$ with respect to the variable X, and σ_Y^2 can be interpreted as a measure of sensitivity of Y with respect to X_i. A detailed analysis procedure of the FOSM method can be found elsewhere [8,18]. Fig. 10 compares the variation of vertical displacement caused by sudden removal of an interior column obtained by the FOSM and Monte Carlo Simulation (MCS) methods, where it can be noticed that the results obtained by the simple FOSM method are similar to those obtained by the more complicated Monte Carlo Simulation method.

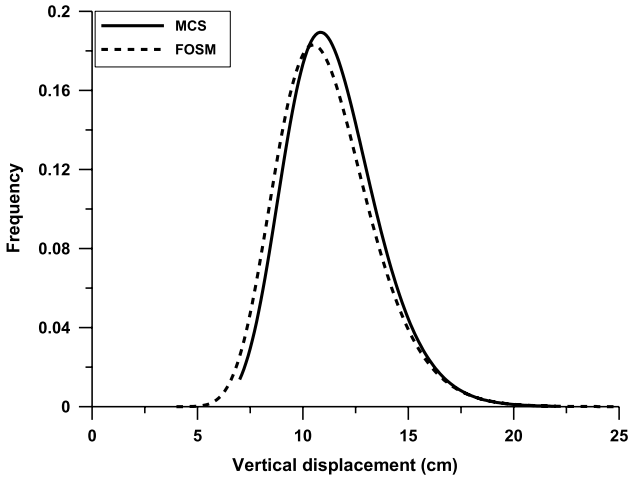

Fig. 10. Variation of vertical displacement of the model structure with WUFB connections subjected to an interior column obtained by FOSM and MCS methods (WUFB connections).

5.3. Fragility curves

Through fragility analysis the probability of failure at various loading states can be obtained. Furthermore, structures can be designed to have a desired probability of failure using the load factor determined from the fragility analysis. For fragility analysis of a structure subjected to progressive collapse under gravity load, the probability for vertical displacement to exceed a given limit state is computed. Fig. 11 depicts the probability density functions of vertical displacement of the model structure having WUFB connections when an interior column was removed. In the analysis, the FOSM method was applied assuming that the mean and the standard deviations had log-normal distribution based on the observation that such an assumption leaded to similar fragility curves obtained by Monte Carlo simulation [19]. The vertical dotted lines represent the vertical displacements corresponding to the IO, LS, and CP limit states. It can be observed that as the

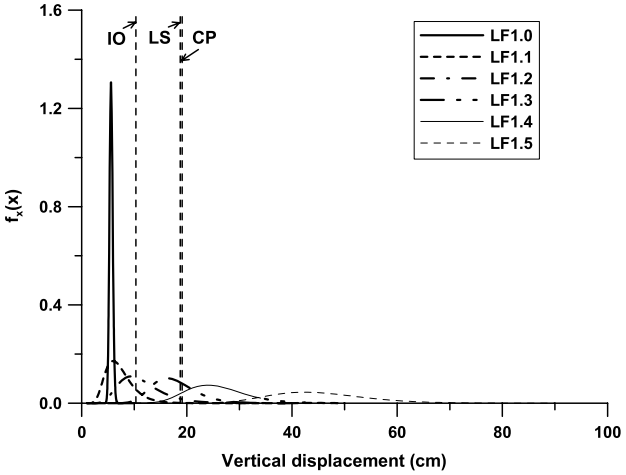

Fig. 11. Probability density functions for vertical displacement of the model structure with an interior column removed for various load factors (WUFB connections).

magnitude of the applied load increased the standard deviation of vertical displacement decreased. In the model structure with WUFB connections subjected to two different vertical loading states, the probability for vertical displacement to exceed a limit state is shown in Table 5. Figs. 12 and 13 show the fragility curves of the model structure with an interior and an exterior column removed, respectively, plotted based on the probability of exceedance of the limit states. It can be observed that the load factor of the structure with the WCPF connections corresponding to a particular limit state is slightly larger than that of the structure with WUFB connections due to the fact that the load resisting capacity of the former is larger than that of the latter. The structure with RBS connections has larger probability of failure at the IO stage, but shows smaller probability of failure at the CP performance level due to the enhanced ductility. Fig. 14 plots the fragility curves of the structure with each connection type at the CP limit state. When an interior column was removed, the structures with WUFB, WCPF, and RBS connections reached 100% probability of exceeding the CP limit states at the load factors of 1.5, 1.6, and 1.7, respectively. When an exterior column was removed, the load factors reduced to approximately 1.2, 1.3, and 1.4, respectively. This implies that the RBS connections have the highest progressive collapse resisting capacity and that the loss of an exterior column is more vulnerable for progressive collapse than the loss of an interior column.

Table 5
Probability of vertical displacement exceeding a limit state.

Load factor	Probability of exceedance		
1.2	0.502	0.044	0.041
1.3	0.949	0.392	0.372

Table 6 presents the load factors of the model structure with three-types of connections corresponding to the 10%, 50%, and 90% probability of failure at the CP state. The load factors obtained by deterministic analysis using the mean values of design variables are also provided for comparison. It can be observed that the load factors obtained from deterministic analyses are similar to those corresponding to the 50% probability of failure.

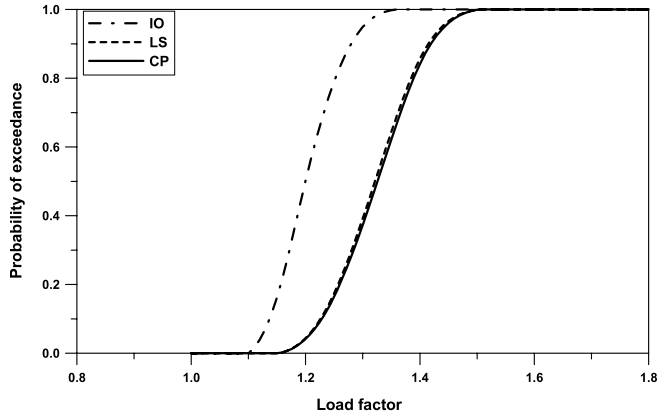

(a) WUFB connections.

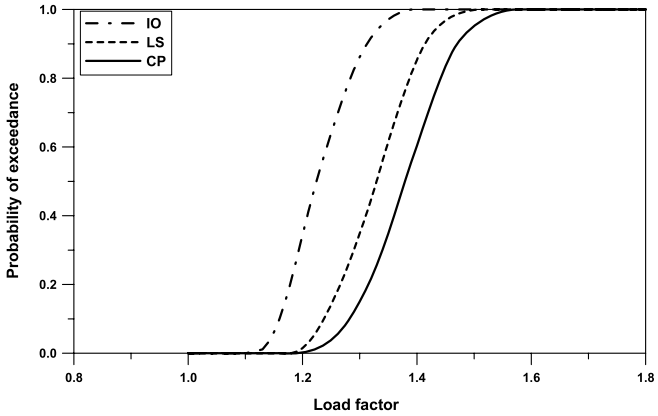

(b) WCPF connections.

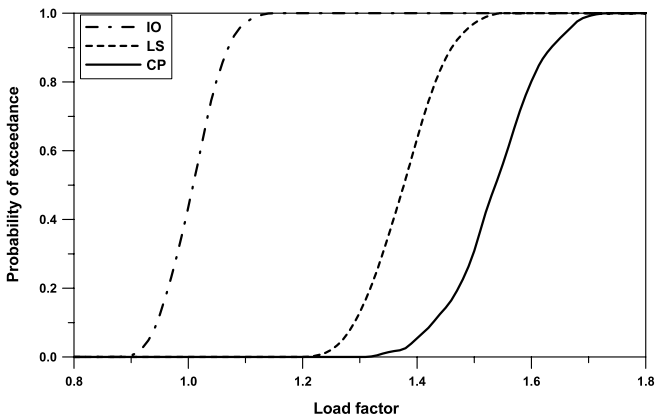

(c) RBS connections.

Fig. 12. Fragility curves of the model structure with an interior column removed corresponding to various limit states.

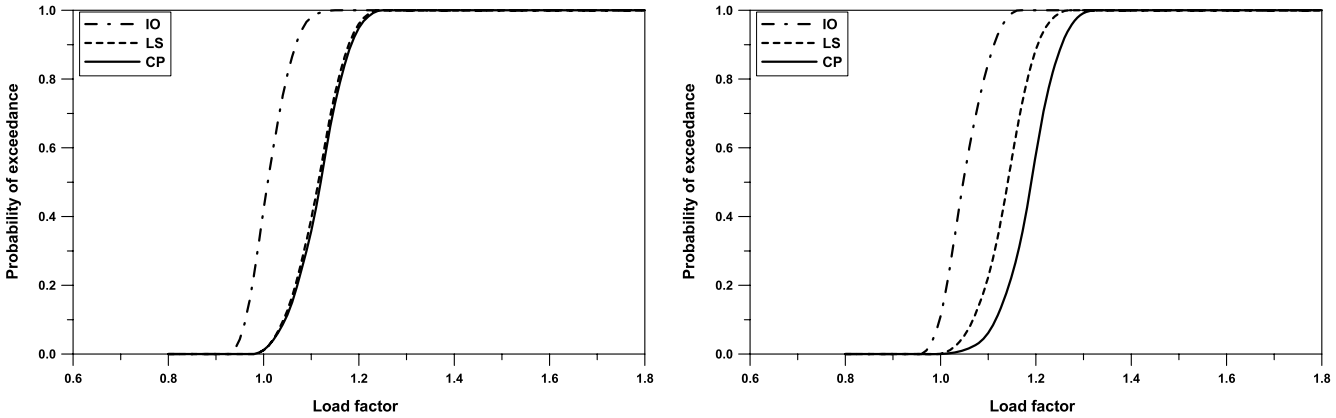

(a) WUFB connections.

(b) WCPF connections.

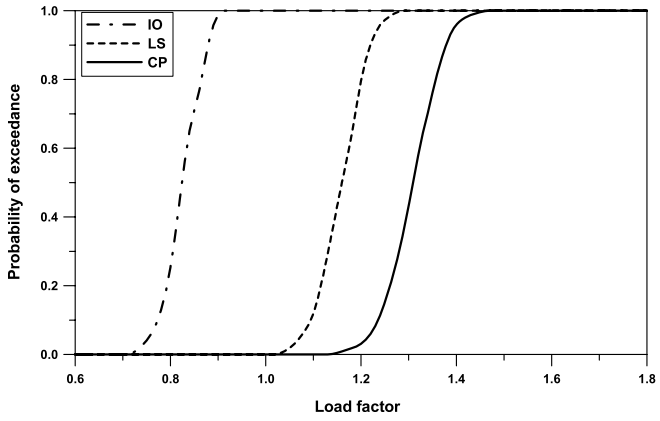

(c) RBS connections.

Fig. 13. Fragility curves of the model structure with an exterior column removed.

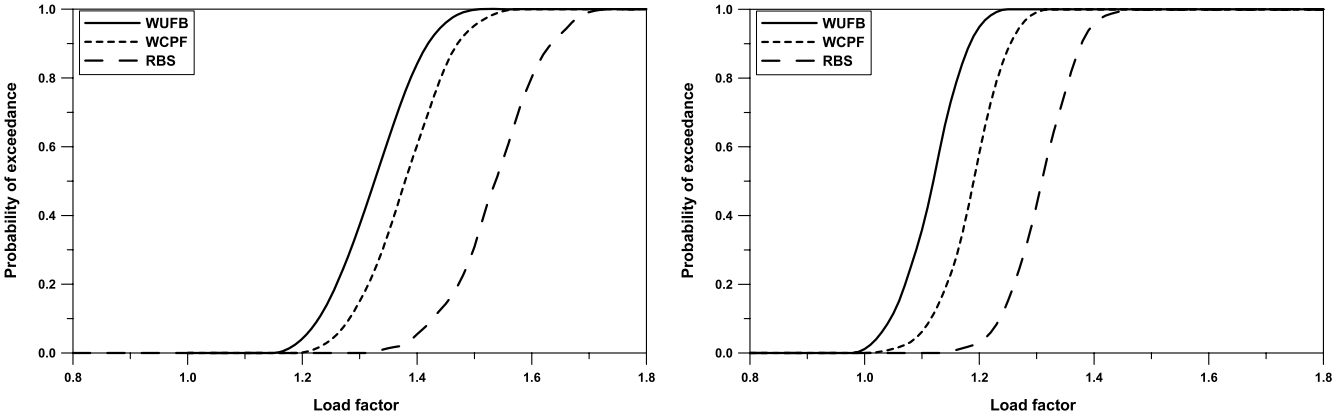

(a) An interior column removed.

(b) An exterior column removed.

Fig. 14. Comparison of fragility curves at CP stage.

Fig. 15 shows the fragility curves of the model structure obtained based on the CP-level limit states of the FEMA-356 and the GSA guidelines when an interior column was removed. The limit states for beam-end rotations and vertical displacements are presented in Table 7. It can be observed that for WUFB and WCPF connections the GSA guidelines specify slightly larger limit states, whereas for RBS connections FEMA-356 provides significantly larger limit states. This resulted in a slightly smaller probability of failure of the WUFB and WCPF connections and a significantly larger probability of failure of the RBS connections when the GSA limit states were applied.

6. Conclusions

Fragility analysis generally provides valuable information on the vulnerability of structures against external load. In this paper fragility analyses of a steel moment frame structure with various connection types such as WUFB, WCPF, and RBS connections were carried out considering variation of design variables such as yield strength, elastic modulus, and live load. The probability of exceeding a given limit state for vertical displacement was obtained using pushdown analysis after removing one of the first-story columns depending on the connection types and the location of the removed column.

Table 6
Load factors at CP state obtained from fragility and deterministic analyses.

(a) Removal of an interior column			
Connection types	Deterministic analysis	Fragility analysis	
	Load factor	Probability of collapse (%)	Load factor
WUFB	1.31	10	1.23
		50	1.32
		90	1.42
WCPF	1.37	10	1.28
		50	1.38
		90	1.47
RBS	1.53	10	1.43
		50	1.54
		90	1.64
(b) Removal of an exterior column			
Connection types	Deterministic analysis	Fragility analysis	
	Load factor	Probability of collapse (%)	Load factor
WUFB	1.12	10	1.04
		50	1.12
		90	1.19
WCPF	1.19	10	1.11
		50	1.19
		90	1.26
RBS	1.31	10	1.22
		50	1.31
		90	1.39

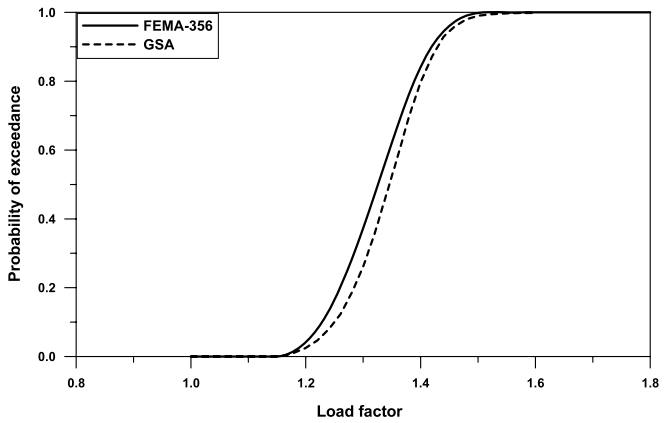

(a) WUFB connections.

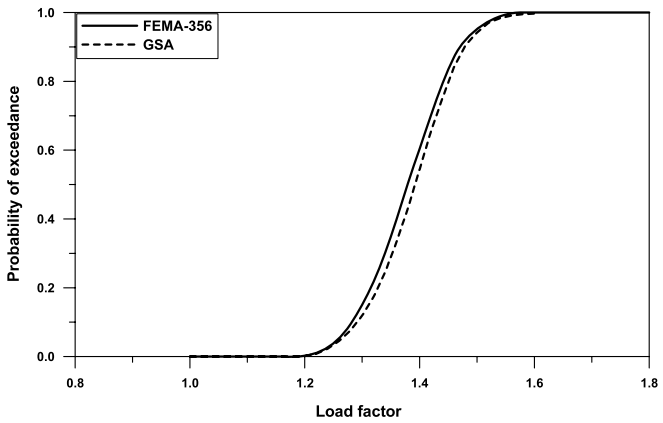

(b) WCPF connections.

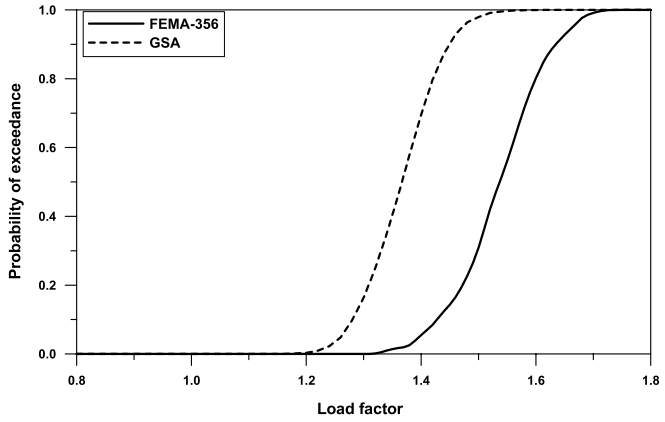

(c) RBS connections.

Fig. 15. Fragility curves based on CP-level limit states of FEMA-356 and GSA guidelines when an interior column was removed.

The analysis results showed that the probability of exceeding the IO limit state was the lowest in the structure with WCPF connections. However, the structure with RBS connections finally had the smallest probability of exceeding the CP limit state owing

Table 7
Comparison of limit states (Interior column removed).

Connection type	GSA		FEMA-356	
	Rotation (rad)	Vertical displacement (cm)	Rotation (rad)	Vertical displacement (cm)
WUFB	0.025	20.56	0.024	19.10
WCPF	0.025	19.05	0.024	18.55
RBS	0.035	50.46	0.047	74.45

to a large ductility capacity. This implies that the structure with RBS connections has the largest progressive collapse resisting capacity when a column is suddenly removed. It was also observed that at 90% probability of exceeding the CP limit state, the load factors ranged between 1.42 and 1.64 when an interior column was removed and between 1.19 and 1.39 when an exterior column was removed. Therefore, when the GSA recommended $2\times$ (dead load + 0.25 live load) is applied as a static load, the model structure with any of the connection types considered in this study may collapse by the sudden removal of a first-story column. It was also observed that the probability of failure of seismic connections depended largely on the limit states provided. Therefore, precise limit states need to be provided for realistic prediction of progressive collapse.

Finally it should be noted that, even though the mechanism of progressive collapse is dynamic in nature, in this study the dynamic effect caused by a suddenly removed column was indirectly considered in the static analyses by the amplification factor of two. It also needs to be mentioned that the probability of collapse would be larger than those obtained in this study if nonseismically designed structures were considered.

Acknowledgement

This research was financially supported by the Super-Tall Building R&D Project of the Ministry of Land, Transport, and Maritime Affairs (09CHUD-A053106-01-000000). The authors are grateful for their support.

References

[1] National institute of standard and technology. Best practices for reducing the potential for progressive collapse in buildings. 2006.
[2] Kim J, An D. Evaluation of progressive collapse potential of steel moment frames considering catenary action. Struct Design Tall Special Build 2009; 18(4):455–65.
[3] Kim T, Kim J, Park J. Investigation of progressive collapse-resisting capability of steel moment frames using push-down analysis. J Perform Constr Fac 2009; 23(5):327–35.
[4] Khandelwal K, El-Tawil S, Sadek F. Progressive collapse analysis of seismically designed steel braced frames. J Constr Steel Res 2009;65:699–708.
[5] Kim J, Kim T. Assessment of progressive collapse-resisting capacity of steel moment frames. J Constr Steel Res 2009;65(1):69–179.
[6] Kim T, Kim J. Progressive collapse-resisting capacity of steel moment frames considering panel zone deformation. Adv Struct Eng 2009;12(2):231–40.
[7] Powell GH, Allahabadi R. Seismic damage prediction by deterministic methods: Concepts and procedures. Earthq Eng Struct Dyn 1988;16(5): 719–34.
[8] Lee TH, Mosalam KM. Probabilistic seismic evaluation of reinforced concrete structural components and systems. PEER Technical Report 2006/04. Berkeley (CA, USA): University of California ; 2006.
[9] Serdar Kircil M, Polat Z. Fragility analysis of mid-rise R/C frame buildings. Eng Struct 2006;28(9):1335–45.
[10] Hueste MBD, Bai JW. Seismic retrofit of a reinforced concrete flat-slab structure: Part II — Seismic fragility analysis. Eng Struct 2007;29(6):1178–88.
[11] Jeong SH, Elnashai AS. Fragility relationships for torsionally-imbalanced buildings using three-dimensional damage characterization. Eng Struct 2007; 29(9):2172–82.
[12] Park J, Towashiraporn P, Craig JI, Goodno BJ. Seismic fragility analysis of low-rise unreinforced masonry structures. Eng Struct 2009;31(1):125–37.
[13] GSA. Progressive collapse analysis and design guidelines for new federal office buildings and major modernization projects. Washington D.C.: The U.S. General Services Administration; 2003.
[14] FEMA-356. Prestandard and commentary for the seismic rehabilitation of buildings. Washington, D.C.: FEMA; 2000.
[15] Krawinkler H, Gupta A, Medina R, Uco N. Loading histories for seismic performance testing of SMRF components and assemblies. SAC/BD-00/10; 2000.
[16] Mazzoni S, McKenna F, Fenves G. Opensees command language manual. Pacific Earthquake Engineering Research (PEER) Center. 2005.
[17] Lee C. Lateral stiffness of steel moment frames with dogbon seismic connections. Comput Struct Eng Inst Korea 2002;15(4):639–47.
[18] Kim T, Kim E, Kim J. Collapse resistance of steel moment connections for gravity load resisting systems. Eng Struct (submitted for publication).
[19] Kim J, Park J, Lee TH. Sensitivity analysis of steel buildings subjected to progressive collapse. Comput Struct Eng Inst Korea 2008;21(2):211–6.
[20] Kim JR, Kim SB, Park YH, Chung WG. Statistical investigation on material properties of SS400 mild steel. Conf Arch Inst Korea 2000;20(1):229–32.
[21] Melchers RE. Structural reliability analysis and prediction. Chichester: John Wiley and Sons; 1999.
[22] Harris ME, Corotis RB, Bova CJ. Area-dependent processes for structural live loads. J Struct Div, ASCE 1981;107(ST5).